

Experimental Study of Effective Parameters in Production of Carbamazepine Nanoparticles

Shadmobaraki, Fariba; Ashraf Talesh, Seyed Siamak*[†]

Department of Chemical Engineering, Faculty of Engineering, University of Guilan, Rasht, I.R. IRAN

ABSTRACT: In this study, confined impinging liquid jets are used to produce nanoparticles of carbamazepine (CBZ). The effect of operating parameters, such as the kind of solvent, CBZ concentration, flow rate of solution and antisolvent on particle size, are experimentally investigated. The Scanning Electron Micrograph (SEM) photomicrographs show that nanodrug with smaller particle is achievable by using solvent with more supersaturation. Meanwhile, decreasing concentration causes the production of smaller particles in the range of 430 to 190 nm and by increasing flow rate of solution, the particle size increases from 240 to 340 nm. Furthermore, the physical states of particles are investigated by Differential Scanning Calorimetry (DSC) test.

KEY WORDS: Carbamazepine; Confined impinging liquid jets; Antisolvent; Nanodrug.

INTRODUCTION

In the pharmaceutical industry, formulation development of poorly water soluble drug represents a challenging problem [1-3]. The main advantages of nanosuspensions are their small particle size and increased surface which in turn lead to increased dissolution rate and improved bioavailability[2,3]. Techniques of drug nanosuspension preparation can be categorized into two principle classes: top-down and bottom-up technologies. The “top-down” technologies are the mechanical processes of larger drug particles, such as milling and homogenization (high-pressure homogenizers). The “bottom-up” technologies begin with the molecules which are dissolved and then precipitated through antisolvent such as SuperCritical Fluid (SCF) technology, spray-freezing into liquid process, Evaporative Precipitation Into aqueous Solution (EPIS) and confined impinging liquid jets [4,5]. It should be mentioned that some drawbacks of “top-down” technologies are time and intensive-energy consumption,

introduction of impurities, inadequate control of particle size and electrostatic effects. So, “bottom-up” technology promotes greater interest toward creation of nanoparticles [1,2,6]. Many techniques have been utilized to reduce the particle size, such as jet-milling, pearl-ball mills, supercritical fluids, spray drying, liquid precipitation, etc. Jet-milling as well as pearl-ball mills is a common way to micronized the particles. However, these techniques show several disadvantages, such as inefficiency due to the high energy input as well as poor control of particle size, morphology and surface properties [1,7-10]. Supercritical fluid techniques and spray drying are believed to be attractive methods for the size reduction, providing particles with narrow size distribution [11-14]. In addition, impinging jets is one of the methods of producing nanodrug particle. In this method, drug solution and antisolvent impinge through two nozzles in which antisolvent is a factor that causes drug particles

* To whom correspondence should be addressed.

+ E-mail: s_ashraf@guilan.ac.ir

1021-9986/15/3/1

9/\$2.90

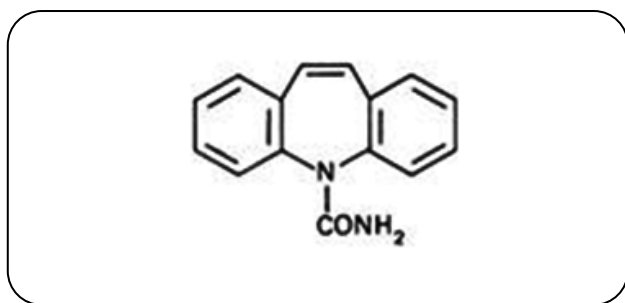


Fig. 1: CBZ molecular structure [10].

precipitate in the form of small particles. As confined liquid impinging jets is a single-pass process; therefore, only mixing can occur. So precipitation of the compound must be completed as soon as possible after mixing. If solute depletion during nucleation and crystal growth is incomplete, secondary crystallization and future growth occur [4-7].

In previous works that have been used on various drugs using bottom-up methods, the effect of parameters, such as concentration, flow rate of solvent, flow rate of anti solvent, temperature, stirring speed, nozzle diameter and the kind of solvent have been studied. Analysis of parameters effect shows that two phenomena of nucleation and growth are important and the crucial crystal properties such as size, morphology and purity are dependent on the rate, largeness and uniformity of supersaturation generated during the process of crystallization [1,3,8]. Moreover, in some methods of bottom-up, such as using impinging jets, residence time has changed by changing flow rate of solvent and antisolvent and has influenced on the phenomena of supersaturation and particles size[5-9].

In this research, the effect of some noted parameters, such as the kind of solvent, concentration, flow rate of solvent and anti solvent to decrease particle size using impinging jets, are investigated.

Carbamazepine is a kind of anti epileptic drug, an anticonvulsant and specific analgesic for trigeminal neuralgia. CBZ is efficient in tonic-clonic seizures acting through the blockade of sodium channels in the neuronal membrane[10]. It is white to off-white powder, almost odorless, exhibits polymorphism, and belonging to the derivatives of dibenzazepine. It works by reducing abnormal electrical activity in the brain. It is characterized by strong lipophilicity; also, about 70–80% of the drug with proteins [11]. Its chemical name and

formula of CBZ are 5H-dibenz azepine-5-carboxamide and C₁₅H₁₂N₂O, respectively. The CBZ molecular structure has been shown in Fig. 1 [10]. It is a drug with low aqueous solubility and high dissolution in alcohol and acetone.

EXPERIMENTAL SECTION

Materials

The raw material of CBZ was provided from Arastoo pharmaceutical company. Methanol and ethanol (purity %99) were purchased from Merck company representation. Deionized water was selected as antisolvent.

Experimental setup

According to Fig. 2, the experimental set up included two peristaltic pumps that the solvent and antisolvent was pumped from opposite directions and impinged in the reactor. The reactor was constructed of two narrow jet with equal diameter and entire process was visible due to the transparent reactor structure. First, the different concentration of drug solution was prepared by mixing raw CBZ in solvents and then impinged by antisolvent in the reactor at various flow rates. The supersaturated mixing of solution-antisolvent stream was added to a deionized water container that with vigorously stirring using a magnetic stirrer was uniform, stable and led to precipitation of particles. After that, the produced sample from above processes was dried and analyzed to achieve its properties [5].

Supersaturation

After impinging antisolvent and drug solution, the nucleation starts. The driving force in nucleation is high and quick supersaturation; which means more nucleation is the result of higher and faster supersaturation [1]. The relation between supersaturation, concentration, and equilibrium solubility is defined as:

$$S = \frac{C}{C_{eq}} \quad (1)$$

Where S, C, and C_{eq} are supersaturation, the actual concentration of CBZ in the solution and the equilibrium solubility of CBZ in mixture of solvent and antisolvent, respectively. It is clear that in a constant drug concentration, the equilibrium solubility intensively decreases, so the supersaturation according to Eq. (1) is increased [12-14].

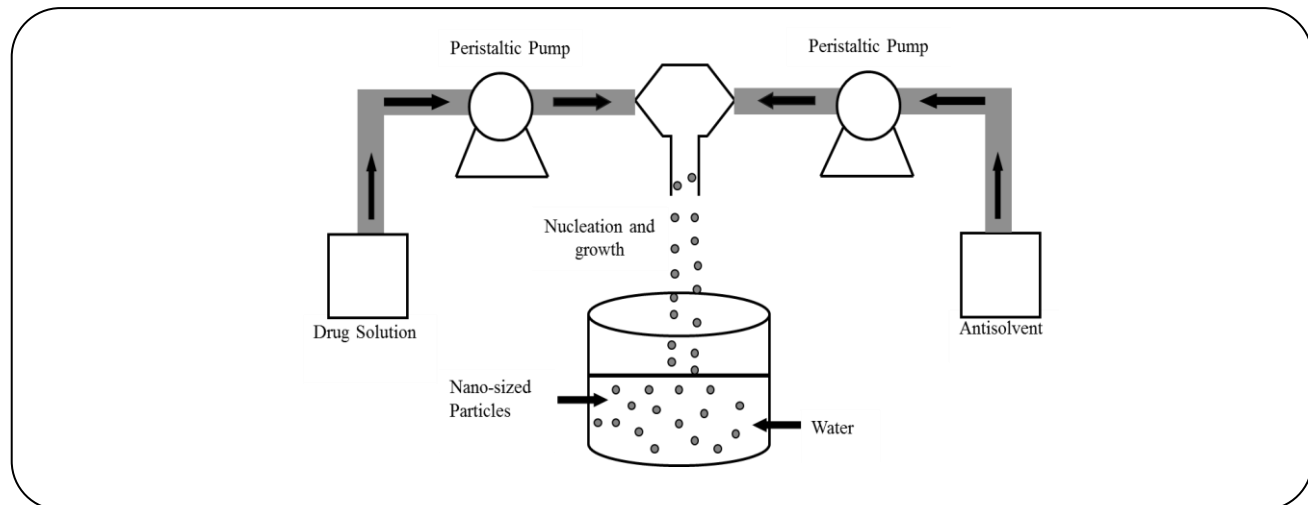


Fig. 2: Schematic diagram of impinging jets set up.

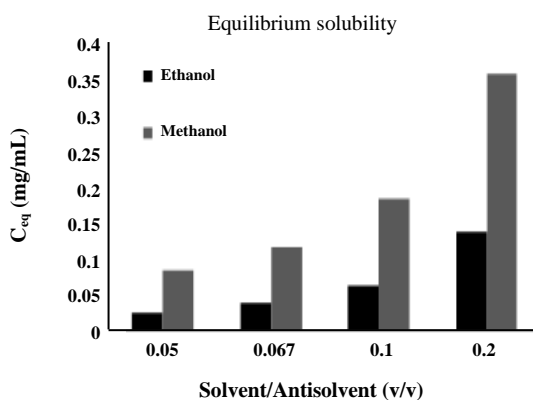


Fig. 3: Equilibrium solubility according to solvent/antisolvent.

In this paper, solubility of CBZ in the solvent and solvent/water mixtures was measured using an UV-based approach. CBZ was added into a beaker containing different ratio of solvent and antisolvent. The obtained solution was stirred for 4h using a magnetic stirrer. A certain amount of sample was filtered, and analyzed by an Agilent UV-visible spectrophotometer.

RESULTS AND DISCUSSION

Some effective parameters, such as kind of solvent, drug concentration, flow rates of solvent and anti solvent are investigated in this study. In the study of effect of solvent kind, methanol and ethanol have been used as solvents and the flow rates of solvent and antisolvent is changed from 20mL/min to 60ml/min and 120mL/min to 160mL/min, respectively.

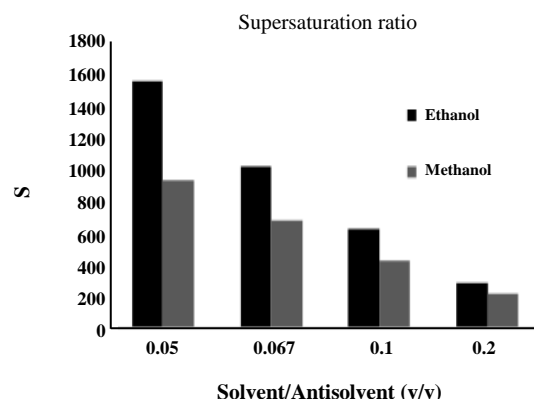


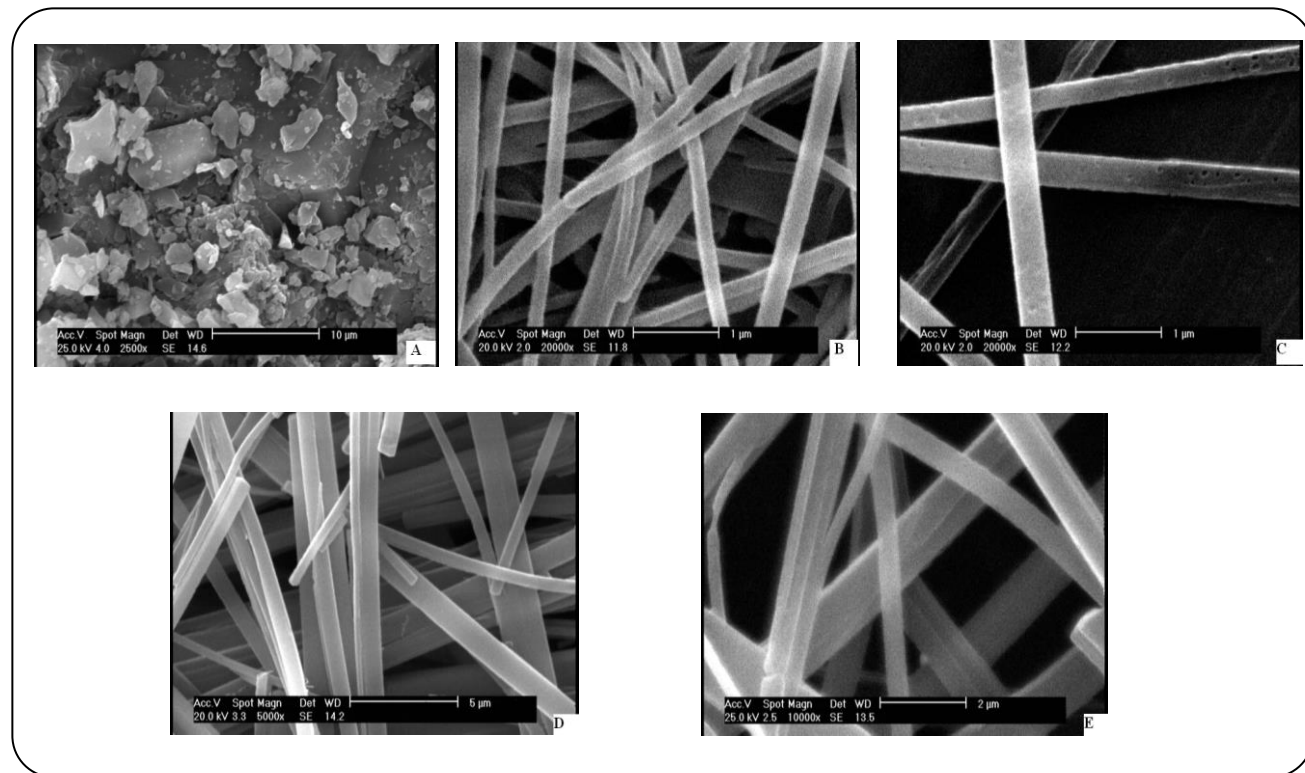
Fig. 4: Supersaturation ratio according to different solvent-antisolvent ratio.

Effect of solvent kind on particle size

In this paper, methanol and ethanol were used as solvents in order to compare the effects of solvents on size and the morphology of particles. Equilibrium solubility and supersaturation of solvents were plotted versus different values of solvent-antisolvent ratio in Figs. 3 & 4, respectively. According to Fig. 3, the equilibrium solubility of drug in both solvents has increased by increasing the solvent-antisolvent ratio. Furthermore, the equilibrium solubility of methanol has been more than the equilibrium solubility of ethanol in the every ratio of solvent-antisolvent. Supersaturation of different solvent-antisolvent system has been calculated based on the values of equilibrium solubility of Fig. 3 using Eq. (1) [1] and has been shown in Fig. 4. It is

Table 1: Effect of kind of solvent.

Average particle size (nm)	Antisolvent volume (mL)	Solution flow rate (mL/min)	Antisolvent flow rate (mL/min)	Sol/anti ratio	Drug concentration (mg/mL)	solvent	Fig. (5)
190	500	60	420	1/7	10	ethanol	B
400	500	60	420	1/7	10	methanol	C
511	500	20	140	1/7	10	ethanol	D
677	500	20	140	1/7	10	methanol	E

**Fig. 5: SEM photographs of (A) unprocessed CBZ; and B, C, D and E, processed CBZ according to Table 1.**

clear from this figure that the supersaturation has decreased with increasing the ratio of solvent-antisolvent.

The supersaturation of the ethanol-deionized water system has been higher than the methanol-deionized water system in every ratio of solvent/antisolvent. The particle size of nano-drugs for two different flow rates of solvents and antisolvent and a constant ratio of Solvent/antisolvent of 1/7 are given in Table 1. The Scanning Electron Micrographs (SEM) of drug before and after jet mixing process based on Table 1 for both solvents have been shown in Fig. 5. It is clear from this figure that ethanol has produced smaller particles than methanol. This results can be achieved by the information

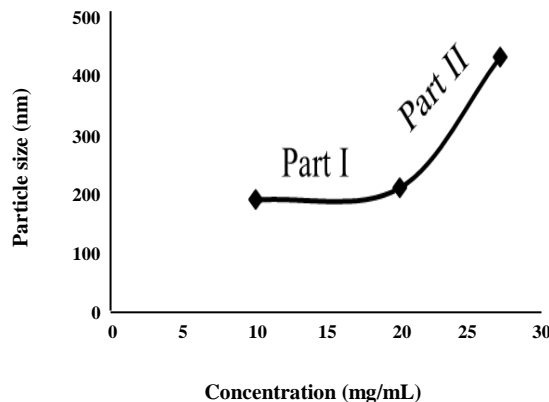
of Fig. 4 according to higher value of supersaturation ratio (S) for ethanol.

Effect of drug concentration

According the mentioned results, ethanol has been produced nanodrugs with smaller particles than methanol; therefore, in this section the effect of concentration of CBZ ethanol solution was used. According to Table 2, the drug concentration varying from 10 to 27 mg/mL has been considered, while other effective parameters, such as solution flow rate, antisolvent flow rate, and Solvent/antisolvent ratio, are fixed. Fig. 6 illustrates the effect of CBZ

Table 2: Effect of concentration.

Average particle size (nm)	Antisolvent volume (mL)	Solution flow rate (mL/min)	Antisolvent flow rate (mL/min)	Sol/anti ratio	Drug concentration (mg/mL)	solvent	Fig. 7
190	500	60	420	1/7	10	ethanol	A
210	500	60	420	1/7	20	ethanol	B
430	500	60	420	1/7	27	ethanol	C

**Fig. 6: Particle size changes versus concentration increases.**

concentration in ethanol/water mixture on the size of particles based on the results of Table 2. It is clear from Fig. 6, the particle size has obviously increased by increasing the CBZ concentration. In addition, the rate of increase in particle size for the first part of this figure is much greater than the second part.

It should be noted that high drug concentration has led high supersaturation which in turn results in a faster nucleation rate and thereby produces nanodrugs with smaller particles. Moreover, particle growth potential increases by higher supersaturation at high drug concentration [15-18]. So the large number of formed nuclei lead to aggregate and formation of larger nanoparticles. On the other hand, the viscosity of drug solution increased with the increasing of concentration, which hindered the diffusion between solution and anti-solvent and thus resulted in non-uniform supersaturation. The same phenomenon was observed by other researchers [14-16]. The SEM micrographs of these experiments are shown in Fig. 7.

Effect of flow rate of both solution and antisolvent

In this section, the effects of flow rate of both solution and antisolvent have been investigated by some experiments which parameters are given in Table 3.

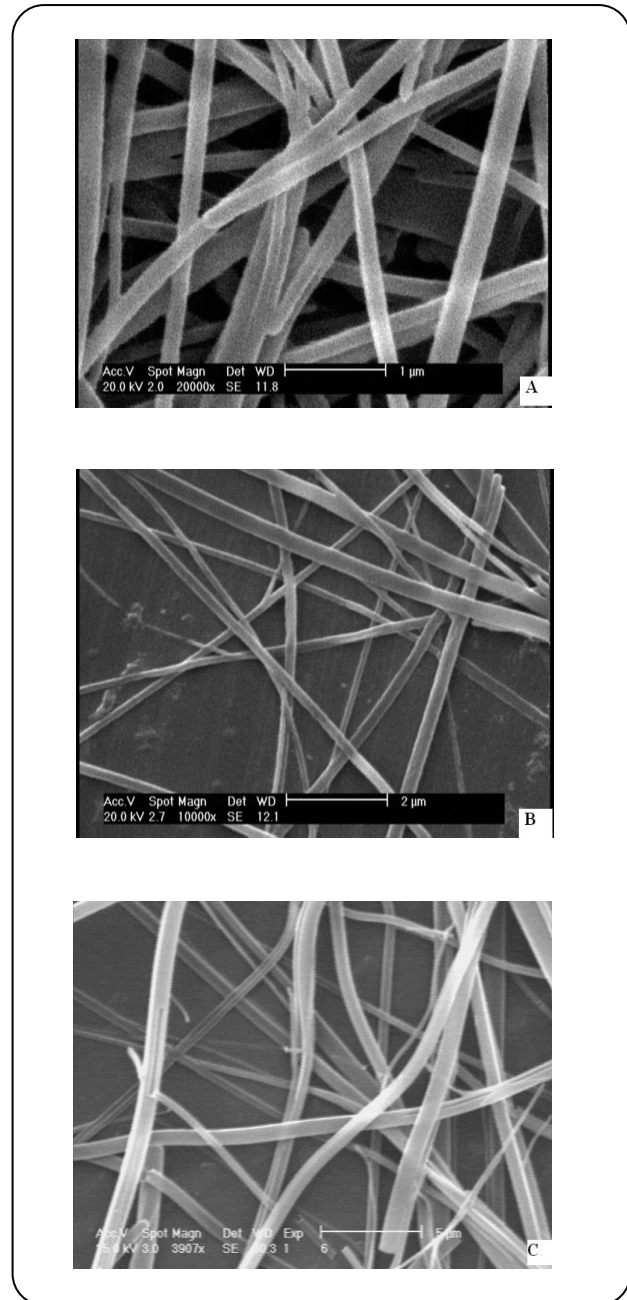
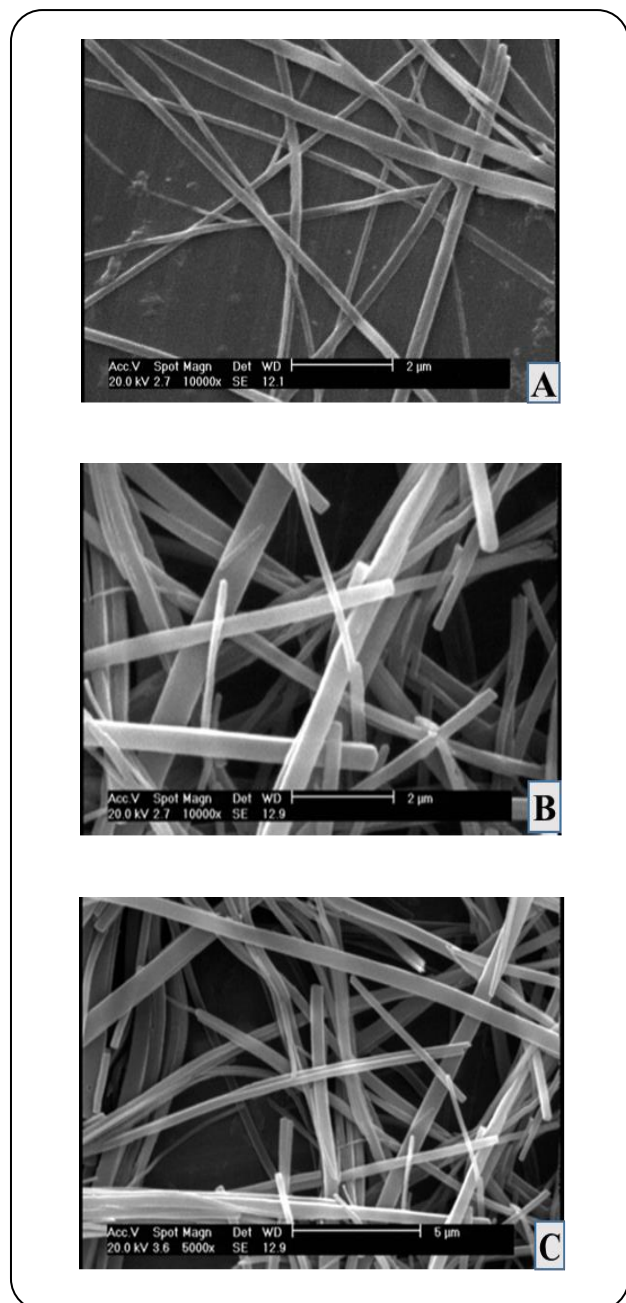
**Fig. 7: SEM photomicrographs of CBZ prepared at different concentration of CBZ (A) 10 mg/mL; (B) 20 mg/mL; (C) 27 mg/mL.**

Table 3: Solution/antisolvent Flow rate effect characteristic.

Average particle size (nm)	Antisolvent volume (mL)	Solution flow rate (mL/min)	Antisolvent flow rate (mL/min)	Sol/anti ratio	Drug concentration (mg/mL)	solvent	Fig. 8
240	500	60	420	1/7	20	ethanol	A
210	500	100	700	1/7	20	ethanol	B
340	500	100	420	1/4.2	20	ethanol	C

**Fig. 8: SEM micrographs of CBZ prepared at different flow rates of CBZ ethanol solution/antisolvent (A) 60:420; (B) 100:700 mL/min; (C) 100:420 mL/min.**

The increasing of flow rates of both solution and antisolvent in an equal ratio of solution/antisolvent (cases (A) and (B) in Table 3) has led nanodrugs with smaller particles. SEM micrographs of these experiments are shown in Figs. 8A and 8B. This behavior is attributed to the higher supersaturation level achieved at higher flow rates due to enhanced mixing [7,12].

It is clear from this table when the overall flow rate has increased from 1/4.2 to 1/7, the particle size has decreased from 340 to 240 nm (case A and C in Table 3). According to Fig. 4, the increasing of ratio of solvent/antisolvent has led to more supersaturation ratio which in turn causes to generate more nuclei in the output of impinging zone. Due to increasing of nucleation, the particle size decreases [18-21].

The Size distribution of particles is an important factor to uniformity behavior of nanodrugs. As can be seen from Fig. 5A, the raw CBZ consists of irregularly shape and completely non-uniform particle size, while for processed CBZ has uniform particle size and regular shape as shown in Fig. 8. The particle size distribution of SEM micrographs of Figs. 8A & 8C is given in Figs. 9A & 9B, respectively.

Based on Fig. 9A, the average particle size has been 240 nm and 95% of the particles have been distributed in the range of 150-350 nm. Fig. 9B shows that average particle size has been 340 nm for SEM picture of Fig. 8C and 97% of the particles have been distributed in the range of 250-550 nm.

DSC test

Fig. 10 shows the thermograms of both the raw (unprocessed) and processed drug nanoparticles acquired by DSC thermal analysis in a range of temperature between 20°C and 200 °C. The samples were equilibrated at 20°C for half an hour to ensure the temperature stability in sample crucible followed by heating at 10°C/min under N₂ atmosphere. The calibration of

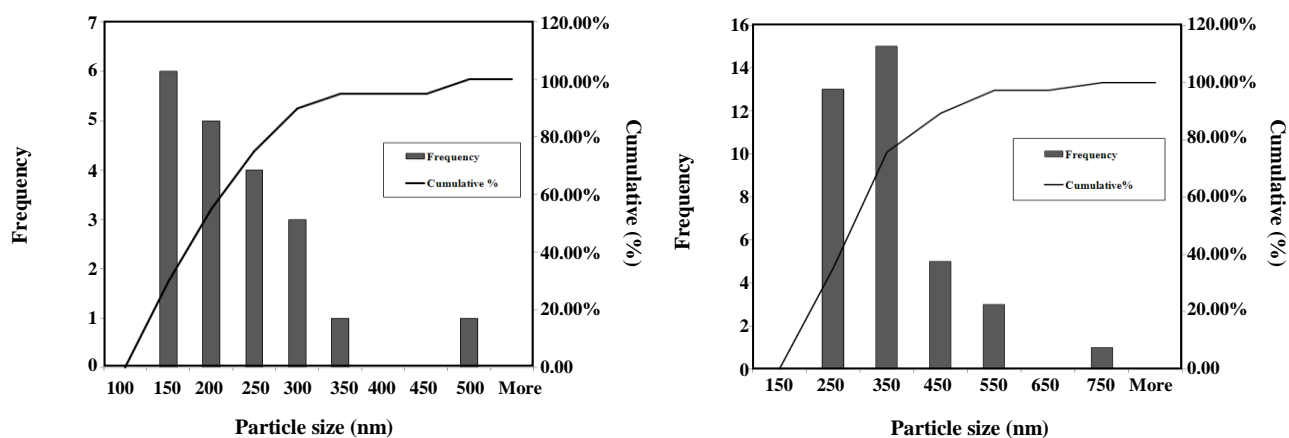


Fig. 9: Histogram and cumulative distribution function of particle size of CBZ for, (A) figure (8B) and, (B) figure (8C).

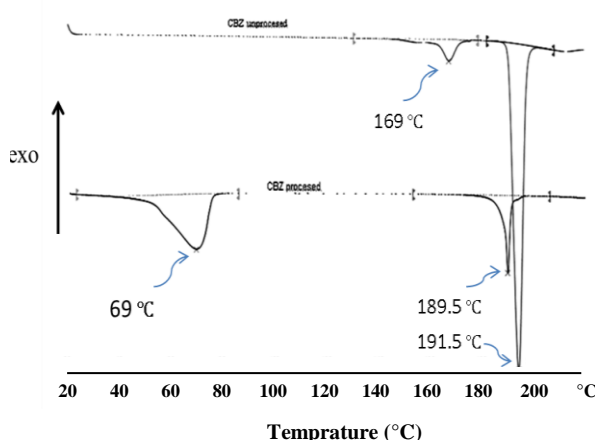


Fig. 10: DSC thermograms of unprocessed (raw) and processed CBZ particles.

temperature and heat flow was performed with standard indium samples.

It is quite evident that the raw CBZ demonstrate a sharp melting peak of bulk CBZ at 191.5°C accompanied with a shallow endothermic peak around 169°C most likely due to impurities imposed by drug synthesis. Moreover the same result has been reported for unprocessed CBZ in [10]. In contrast, the processed CBZ nanoparticles show a melting endotherm about 189.5°C with dramatic decrease in peak area. The modest decrease in melting point occurrence can be attributed to smaller particle size for CBZ material after processing. The significant decrease in peak area for processed CBZ also supports the hypothesis of lower particle size for processes material. In addition, this phenomena can be explained by the fact that the higher nucleation rate,

the lower time available for particle incorporation while crystal lattice growing. As a consequence, the lower peak area can be expected as it has been reported in literature [10, 23-25]. Moreover, the peak depletion at 169 °C for processed CBZ is a good evidence for effective removal of impurities during treatment process. It is worth to note that the treatment process imposes a solvent residue which indicates by an evident broad endothermic peak around 69.4°C.

CONCLUSIONS

In this study, first ethanol and methanol have been used as solvents for the production of CBZ nanoparticle. Since the solubility of ethanol is higher than methanol, by increasing supersaturation (in CBZ ethanol solution), particle size has decreased according to SEM micrographs. It has been shown that the average particle size of CBZ has significantly increased from 190 to 430nm by concentration increase and the solution flow rate. The particle size decreased from 340 to 240nm by increasing in solution/antisolvent ratio. The DSC test has been shown that the melting points and the peak height of produced nanoparticles have decreased, so particle crystalline structure for produced nanoparticles has decreased.

Acknowledgment

The authors kindly thank to the Iran's Arastoo Pharmaceutical Manufacture Company for supplying the carbamazepine drug.

Received : June 1, 2014 ; Accepted : Apr. 27, 2015

REFERENCES

- [1] Thorat A.A., Dalvi S.V., Liquid Antisolvent Precipitation and Stabilization of Nanoparticles of Poorly Water Soluble Drugs in Aqueous Suspensions: Recent Developments and Future Perspective, *Chemical Engineering Journal*, **181**: 1-34 (2012).
- [2] Lipinski Ch.A., Drug-Like Properties and the Causes of Poor Solubility and Poor Permeability, *Journal of Pharmacological and Toxicological Methods*, **44**: 235-249 (2000).
- [3] Ba-Abbad M.M., Kadhum A.A.H., Mohamad A.B., Takriff M.S., Sopian K., Optimization of Process Parameters using D-Optimal Design for Synthesis of ZnO Nanoparticles via Sol-Gel Technique, *Journal of Industrial and Engineering Chemistry*, **19**(1): 99-105 (2013).
- [4] Ali H.S.M., York P., Blagden N., Preparation of Hydrocortisone Nanosuspension Through a Bottom-up Nano Precipitation Technique Using Microfluidic Reactors, *International Journal of Pharmaceutics*, **375**: 107-113 (2009).
- [5] Bazdidi-Tehrani F., Imanifar A., Khajehhasani S., Rajabi-Zargarabadi M., Normal-Velocity Relaxation and Higher Order Algebraic Heat Flux Models Applicable to an Axisymmetric Impinging Jet, *Journal of Dispersion Science and Technology*, **33**: 556-564 (2012).
- [6] Alaei M., Mahjoub A.R., Rashidi A., Preparation of Different WO₃ Nanostructures and Comparison of Their Ability for Congo Red Photo Degradation, *Iranian Journal Chemistry and Chemical Engineering (IJCCE)*, **31**: 31-36 (2012).
- [7] Chiou H., Chan H.-K., Heng D., Prud'homme R.K., Raper J.A., A Novel Production Method for Inhalable Cyclosporine A Powders by Confined Liquid Impinging jet Precipitation, *Journal of Aerosol Science*, **39**: 500-509 (2008).
- [8] Saiei J., Ojaghi S.A., Effect of Aqueous Phase pH on Liquid-Liquid Extraction with Impinging-Jets Contacting Technique, *Journal of Industrial and Engineering Chemistry*, **16**:1001-1005 (2010).
- [9] Homaunmir V., Tohidi S.H., Grigoryan G., Characterization of Sol-Gel Derived CuO@SiO₂ Nano Catalysts towards Gas Phase Reactions, *Iranian Journal Chemistry and Chemical Engineering (IJCCE)*, **32**: 37-44 (2013).
- [10] Park M.-W., Yeo S.-D., Antisolvent Crystallization of Carbamazepine from Organic Solutions, *Chemical Engineering Research and Design*, **90**: 2202-2208 (2012).
- [11] Patel R.B., Patel M.R., Bhatt K.K., Patel B.G., Formulation Consideration and Characterization of Microemulsion Drug Delivery System for Transnasal Administration of Carbamazepine, *Bulletin of Faculty of Pharmacy, Cairo University*, **51**: 243-253 (2013).
- [12] Beck Ch., Dalvi S.V., Dave R.N., Controlled Liquid Antisolvent Precipitation using A Rapid Mixing Device, *Chemical Engineering Science*, **65**: 5669-5675 (2010).
- [13] Ali H.M.S., Blagden N., York P., Amani A., Brook T., Artificial Neural Networks Modelling the Prednisolone Nanoprecipitation in Microfluidic Reactors, *European Journal of Pharmaceutical Science*, **37**: 514-522 (2009).
- [14] Zhang J.-Y., Shen Z.-G., Zhong J., Hu T.-T., Chen J.-F., Ma Z.-Q., Yun J., Preparation of Amorphous Cefuroxime Axetil Nanoparticles by Nanoprecipitation Method without Surfactants, *International Journal of Pharmaceutics*, **323**: 153-160 (2006).
- [15] Ghaffarian H.R., Saiedi M., Sayyadnejad M.A., Rashidi A.M., Synthesis of ZnO Nanoparticles by Spray Pyrolysis Method, *Iranian Journal Chemistry and Chemical Engineering (IJCCE)*, **30**: 1-6 (2011).
- [16] Chan H.-K., Kwok Ph.Ch.L., Production Methods for Nanodrug Particles Using the Bottom-Upapproach, *Advanced Drug Delivery Reviews*, **63**: 406-416 (2011).
- [17] Zhang H.-X., Wang J.-X., Shao L., Chen J.-F., Microfluidic Fabrication of Monodispersed Pharmaceutical Colloidal Spheres of Atorvastatin Calcium with Tunable Sizes, *Industrial and Engineering Chemistry Research*, **49**: 4156-4161 (2010).
- [18] Zabihi F., Akbarnejad M.M., Vaziri Yazdi A., Arjomand M., Safekordi A.A., Drug Nano-Particles Formation by Supercritical Rapid Expansion Method; Operational Condition Effects Investigation, *Iranian Journal Chemistry and Chemical Engineering (IJCCE)*, **30**: 7-15 (2011).
- [19] Dong Y., Ng W.K., Hu J., Shen Sh., Tan R.B.H., A Continuous and Highly Effective Static Mixing Process for Antisolvent Precipitation of Nanoparticles of Poorly Water-Soluble Drugs, *International Journal of Pharmaceutics*, **386**: 256-261 (2010).

- [20] Wang Z., Chen J.-F., Le Y., Shen Z.-G., Preparation of Ultrafine Beclomethasone Dipropionate Drug Powder by Antisolvent Precipitation, *Industrial and Engineering Chemistry Research*, **46**: 4839-4845 (2007).
- [21] Dong Y., Ng W.K., Shen Sh., Kim S., Tan R.B.H., Preparation and Characterization of Spironolactone Nanoparticles by Antisolvent Precipitation, *International Journal of Pharmaceutics*, **375**: 84-88 (2009).
- [22] Dalvi S.V., Dave R.N., Analysis of Nucleation Kinetics of Poorly Water-Soluble Drugs in Presence of Ultrasound and Hydroxypropyl Methyl Cellulose During Antisolvent Precipitation, *International Journal of Pharmaceutics*, **387**: 172–179 (2010).
- [23] S.M. Ali H., York P., M.A. Ali A., Blagden, N., Hydrocortisone Nanosuspensions for Ophthalmic Delivery: A Comparative Study between Microfluidic Nanoprecipitation and Wet Milling, *Journal of Controlled Release*, **149**: 175-181 (2011).
- [24] El-Gendy N., L. Aillon K., Berkland C., Dry Powdered Aerosols of Diatrizoic Acid Nanoparticle Agglomerates as a Lungcontrast Agent, *International Journal of Pharmaceutics*, **39**: 305-312 (2010).
- [25] Matteucci M.E., Hotze M.A., Johnston K.P., Williams R.O., Drug Nanoparticles by Antisolvent Precipitation: Mixing Energy Versus Surfactant Stabilization, *Langmuir*, **22**: 8951-8959 (2006).